Functional and cytometric examination of different human lung epithelial cell types as drug transport barriers

Kyoung Ah Min[1,2], **Gus R. Rosania**[2], **Chong-Kook Kim**[3], and **Meong Cheol Shin**[1,*]

[1]College of Pharmacy and Research Institute of Pharmaceutical Sciences, Gyeongsang National University, 501 Jinju Daero, Jinju, Gyeongnam 52828, Republic of Korea

[2]Department of Pharmaceutical Sciences, College of Pharmacy, University of Michigan, 428 Church St., Ann Arbor, MI 48109, USA

[3]College of Pharmacy, Seoul National University, 1 Gwanak-ro, Gwanak-gu, Seoul 08826, Republic of Korea

Abstract

To develop inhaled medications, various cell culture models have been used to examine the transcellular transport or cellular uptake properties of small molecules. For the reproducible high throughput screening of the inhaled drug candidates, a further verification of cell architectures as drug transport barriers can contribute to establishing appropriate *in vitro* cell models. In the present study, side-by-side experiments were performed to compare the structure and transport function of three lung epithelial cells (Calu-3, normal human bronchial primary cells (NHBE), and NL-20). The cells were cultured on the nucleopore membranes in the air-liquid interface (ALI) culture conditions, with cell culture medium in the basolateral side only, starting from day 1. In transport assays, paracellular transport across all three types of cells appeared to be markedly different with the NHBE or Calu-3 cells, showing low paracellular permeability and high TEER values, while the NL-20 cells showed high paracellular permeability and low TEER. Quantitative image analysis of the confocal microscope sections further confirmed that the Calu-3 cells formed intact cell monolayers in contrast to the NHBE and NL-20 cells with multilayers. Among three lung epithelial cell types, the Calu-3 cell cultures under the ALI condition showed optimal cytometric features for mimicking the biophysical characteristics of *in vivo* airway epithelium. Therefore, the Calu-3 cell monolayers could be used as functional cell barriers for the lung-targeted drug transport studies.

---

*Corresponding author: Meong Cheol Shin, Ph.D., shinmc@gnu.ac.kr; Tel.: +82-55-772-2421; Fax: +82-55-772-2429. College of Pharmacy and Research Institute of Pharmaceutical Sciences, Gyeongsang National University, 501 Jinju Daero, Jinju, Gyeongnam 52828, Republic of Korea.

Introduction

In the field of pharmaceutical sciences, the *in vitro* cell models are advantageous for high throughput screening of drug development due to their simple and reproducible systems (Bhadriraju and Chen 2002; Astashkina et al. 2012). Caco-2, or MDCK cells have been widely used in pharmacokinetic studies for oral drug development because of their unique characteristics to form tight junctions with cell monolayers on the porous supports which enable to examine oral drug absorption or metabolism, mimicking the *in vivo* intestine (Irvine et al. 1999; Shah et al. 2006; Volpe 2008). While these cells are still first-choice *in vitro* models for oral drug delivery, they may not have appropriate physiological characteristics to study lung delivery that is also an important route of drug administration. There has been substantial research on lung delivery for local or systemic therapy (Agu et al. 2001; Gonda 2006; Patton and Byron 2007) and many previous investigations have been devoted to characterization of human lung epithelial cells (Gray et al. 1996; Forbes and Ehrhardt 2005).

Due to the formation of cell monolayers on the porous membrane with tight junctions compatible with the *in vivo* system, Calu-3 (human bronchial adenocarcinoma cell lines) are a representative *in vitro* model to study lung absorption and distribution (Grainger et al. 2006). Various pharmacokinetic studies, such as drug absorption, distribution, metabolism (transporters or enzymes), and toxicity have been performed with the Calu-3 cells (Florea et al. 2003). The Calu-3 cells are immortalized cells, because their origins are bronchial adenocarcinoma, resulting in an easy culture with low costs (Shen et al. 1994). On the other hand, primary cells can show lung physiology similar to *in vivo* lung (Gray et al. 1996); however, they might have disadvantages in the *in vitro* cultures because, as compared to the Calu-3 cells, experienced techniques should be necessary to obtain primary cells from an organism with relatively high costs, and they can be alive in a specialized culture environment only in a definite period (Wu et al. 1997; Sachs et al. 2003).

Nonetheless, NHBE (normal human bronchial epithelial cells) are a type of primary cells that are easily obtained commercially. As reported in previous studies, they can be grown on the porous supports with tight junctions (Lin et al. 2007; Yu et al. 2012). As a unique cell type in the middle of cancer-origin cells and primary cells, transformed cells can be useful for the studies because they are immortalized by transfection methods and their physiology might be closer to that of primary cells than to that of cancer-derived cells (Cozens et al. 1992). NL-20 (human bronchial transformed epithelial cells) are a type of transformed lung epithelial cell lines obtained by transfection with the origin of replication-defective SV40 large T plasmid (Schiller et al. 1992). However, further research is needed on their function as transport barriers. In order to utilize the pharmacokinetic data from the cell studies to be compatible with those from the *in vivo* model, the *in vitro* experimental system needs to be characterized by various scopes.

In the present study, three different human bronchial epithelial cells were characterized as functional cell barriers for drug transport and were then compared in morphology by imaging analyses with biochemical probes. These cells were cultured on polyester membrane supports under the ALI (air-liquid interface) culture condition with ambient air

on the apical side and only medium on the basolateral side, which mimics the environment in the physiological lung with gas exchanges. Since the intactness of the confluent cell layers on the membrane is an essential standard of a functional barrier for drug transport, the changes of transepithelial electrical resistance (TEER) values were followed up for three different cell types throughout the days of ALI cultures. Moreover, Lucifer yellow (LY), a hydrophilic compound, was used as a paracellular transport marker to examine the intactness of the cell layers on the membrane. As another way to characterize the cell layers grown on the porous membrane structure, confocal 3D imaging was performed to compare the three cell types in terms of cell morphologies, as well as transport and distribution of cell-permeant dye molecules.

The hypothesis investigated in this study is that cell 3D architectures of different lung epithelial cells on the porous supports would affect the permeability or intracellular accumulation of small molecules. Our biophysical approach to cell characterization would provide a better understanding of three types of human lung epithelial cells with the morphological parameters such as cell size or volume and, furthermore, of desirable properties as cell models for the inhaled drug transport studies and development.

Materials and methods

Materials

All chemicals to prepare Hank's balanced salt solution (HBSS) were purchased from Fisher Scientific, Inc. (Pittsburgh, PA). The supplements for the complete growth medium of NL-20, such as epidermal growth factor (EGF), hydrocortisone, D-(+)-glucose solution (10%), and sodium bicarbonate solution (7.5%), were obtained from Sigma Life Science (St. Louis, MO). BEGM bullet kit and subculture reagent for the NHBE cells were purchased from Lonza co (Walkersville, MD). All other compositions for the cell cultures including Dulbecco's Modified Eagle Medium: Nutrient Mixture F-12 (DMEM: F12) were obtained from Invitrogen, Co. (Carlsbad, CA). MitoTracker® Red CMXRos (M7512), LysoTracker® Green DND-26 (L7526), and Hoechst 33342 (H3570) were purchased from Molecular Probes, Invitrogen. Lucifer yellow CH dipotassium salt (Molecular weight: 521.57) was purchased from Sigma-Aldrich (St. Louis, MO). Transwell™ inserts (area 0.33 cm^2, pore size: 0.4 or 3 μm) were obtained from Corning Co. (Lowell, MA).

Cell culture

The Calu-3 and NL-20 cells were obtained from the American Type Culture Collection (ATCC) (Manassas, VA) and cultured in 75 cm^2 flasks at 37°C in a 95% air/5% CO_2 humidified incubator according to the manufacturer's protocols. The Calu-3 cells were maintained in media containing the 1:1 mixture of Dulbecco's Modified Eagle Medium and Nutrient mixture F12 (DMEM:F12) with 2 mM L-glutamine, 1% (v/v) non-essential amino acids, 1% (v/v) penicillin-Streptomycin, and 10% fetal bovine serum (FBS; Gibco# 10082). The NL-20 cells were grown in Ham's F12 medium with supplements (1.5 g/l sodium bicarbonate, 2.7 g/l glucose, 2mM L-glutamine, 1% (v/v) non-essential amino acids, 1% (v/v) Insulin-Transferrin-Selenium-X, 10 ng/ml EGF, 500 ng/ml hydrocortisone, and 4% FBS).

The NHBE cells (Clonetics™) were cultured in the BEGM medium containing serum-free medium BEBM with supplements (human recombinant epidermal growth factor, insulin, transferrin, hydrocortisone, triiodothyronine, epinephrine, retinoic acid, gentamycin/amphotericin-B, and bovine pituitary extract) in the bullet kit. Culture media in flask were changed every second day during the cultures. After reaching confluency, the Calu-3, NHBE, and NL-20 cells were transferred into the culture flasks by using 0.125% Trypsin-EDTA at the 1:3, 1:6, and 1:12 split ratio, respectively, for the continuous cultures.

Transwell™ insert cultures of lung cells under the ALI condition

For transport experiments and confocal image analyses of lung epithelial cells, each cell type was seeded at the optimal cell density (Calu-3: 5×10^5 cells/cm^2, NHBE: 2.5×10^5 cells/cm^2, NL-20: 1.5×10^5 cells/cm^2) on 0.33 cm^2 polyester Transwell™ inserts and then maintained with culture media of each cell type on the apical and basolateral sides at 37 °C in a humidified 5% CO_2 incubator. After overnight culture of the Calu-3, NHBE or NL-20 cells in inserts, the cell attachment on the polyester membrane was examined by light contrast inverted Nikon TE2000 microscope. Media on the apical side in the Transwell™ culture of the cells were aspirated and the apical sides were washed by the HBSS buffer (10 mM HEPES, 25 mM D-glucose, pH 7.4) to remove the unattached cells from the membranes. Media on the basolateral sides were replaced with fresh media every day for the Air-Liquid Interface Culture (ALI) culture, while the cells were maintained at 37°C in a humidified 5% CO_2 incubator.

Transepithelial electrical resistance (TEER) measurement

During the ALI cultures (20 days) of each lung cell type (Calu-3, NHBE, and NL-20) in the Transwell™ inserts, the integrities of cell layers were examined by the transepithelial electrical resistance (TEER) measurements (see the diagram in Fig. 1). The media on the apical and basolateral sides in the inserts with the cells were pre-equilibrated for 20 min at 37°C in a 5% CO_2 incubator. To measure the TEER values of the cell layers, the electrode pairs of the Millipore Millicell® ERS were submerged into the media in the apical and basolateral chambers of the inserts in the 24-well plates. The TEER values ($\Omega \cdot cm^2$) of the cell layers were corrected by subtracting the blank TEER values (without the cells) in the inserts with the media in both chambers and by considering the area of the porous membranes of the inserts (0.33 μm^2).

LY transport assessment

Lucifer yellow (LY) was utilized as a marker of the paracellular transport in the cell layers in Transwell™ inserts. In addition to the TEER measurements, permeability of LY was measured with the 24-well Transwell inserts with the cells to examine the intactness of the cell layers. The inserts with the Calu-3, NHBE, and NL-20 cells on day 8 when these cell-types showed plateau of the TEER values or formed the stable cell layers with confluency were used for the LY transport experiments. Three cell types were further assessed for the different degrees of tight junction formation of differentiated cell layers during the ALI cultures on the inserts by the LY permeability measurements. On day 8, referring to our previously reported methods (Suresh et al. 2012), transport experiments were performed with both directions, i.e. the apical-to-basolateral (AP→BL) and the basolateral-to-apical

(BL→AP) for these different cell type cultures. One millimolar LY solution in the transport buffer (HBSS) was added onto the apical (donor) sides of the cells in the inserts, as there was an LY-free transport buffer on the basolateral (receiver) sides for the AP→BL transport. On the other hand, for the BL→AP transport, 1mM LY solution was added onto the basolateral (donor) sides while there was only a buffer on the apical (receiver) sides.

The LY transport experiments were performed for 180 min under a stirring condition by the VWR rocking platform shakers. During the experiments, sample solutions were collected from the receiver sides at each time point (0, 5, 10, 30, 60, 90, 120, 150, and 180 min) and the donor side at the end time point. The fluorescence signals of LY in the standard and sample solutions were measured at 485 nm (excitation)/540 nm (emission) by the plate reader (BioTEK® Synergy™ BioTEK, Co.). For the AP→BL or BL→AP transport, the transcellular permeability coefficient, P_{eff} (cm/sec), was calculated by normalizing the AP→BL or BL→AP mass transport rate with the insert area (0.33 cm^2) and the initial LY concentration (Suresh et al. 2012).

Confocal microscopic imaging

In order to assess the architectures of the different types of lung cells on the polyester membranes in the Transwell™ inserts, the cells seeded on the membranes at the optimal cell density (Calu-3: 5×10^5 cells/cm^2, NHBE: 2.5×10^5 cells/cm^2, NL-20: 1.5×10^5 cells/cm^2) were cultured under the ALI conditions with the media on only basolateral sides for further confocal image analysis. The cells on the membranes were maintained after seeding at 37°C in a 95% air/5% CO$_2$ humidified incubator until day 20 and then were examined by Zeiss LSM 510-META laser scanning confocal microscope (Carl Zeiss Inc., Thornwood, NJ) with a $60 \times$ water immersion objectives on different days of cultures under the ALI conditions. For the confocal analyses, three different dyes were prepared by dilution with the HBSS buffer (10 μg/ml Hoechst 33342 (HOE), 2.5 μM LysoTracker® Green DND-26 (LTG), and 1 μM MitoTracker® Red (MTR)).

After the apical and basolateral sides of the cell layers on the membranes were washed twice by the transport buffer (HBSS), 240 μl of the dye mixtures (80 μl of each dye) in HBSS were put onto the apical sides, while there was 600 μl of dye-free buffer on the basolateral sides. The cells in the inserts were incubated at 37°C in 5% CO$_2$ incubator for 30 min and the inserts were put directly onto two-well Lab-Tek® chambered #1 borosilicate cover-glasses (Thermo Scientific Nunc Co.). Without any fixations, the confocal imaging of the live cells on the insert was performed using laser for UV (364 nm), argon laser (488 nm), and helium neon 1 laser (543 nm). The obtained cell images were analyzed along the Z-axis (interval, 1 μm) in three fluorescence channels.

Cytometric analysis of cell architecture

Cellular morphometric parameters, such cell size, height, and volume, were measured by using MetaMorph image analysis software (Molecular Devices, Sunnyvale, CA) based on confocal 3D images of three lung cell types in the inserts. For the fluorescent images of the Calu-3, NHBE, and NL-20 cells on the membranes, each Z-stack image underwent background subtraction and thresholding algorithm in the software. Sizes of the cells on

each image plane were measured by the "Region measurement" function. Cell height was calculated by adding z-intervals to Z-stacks of images. By assuming a polyhedron shape of the cell, cell volume was obtained from the sums of the segmented cell areas along z-axis of 1 μm spacing, as suggested by the previously reported method (Frixione et al. 2001). This cytometric analysis was performed for three different batches of confocal images for each cell type.

Statistical analysis

GraphPad Prism 5.0 was used to generate plots with statistical analysis. Box plots showing median and interquartile range with whisker ends were depicted after the post-hoc multiple mean comparison (Tukey's test, $p<0.05$).

Results

Functional analysis

Cell layer formation in Transwell™ inserts under ALI culture condition—In the experimental setup with the Transwell™ inserts (see the diagram in Fig. 1B), intactness of the confluent cell layers on the membrane was checked by measuring the TEER values for these bronchial epithelial cell models (Calu-3, NHBE or NL-20) throughout the days of the ALI cultures (Fig. 1A). The ALI conditioned culture started on day 1 by apical medium removed and TEER values were measured from day 1 to day 20. Initially, the Calu-3 cells had low average TEER values, such as 97 $\Omega \cdot cm^2$ ($\pm$ 6.23, standard deviation (S.D.)) on day 3. After day 6 of cultures, the TEER values increased to over 350 $\Omega \cdot cm^2$, which is a standard TEER value for the confluent Calu-3 monolayers with appropriate intactness (Borchard et al. 2002). Between days 6 and 20, the Calu-3 cells showed consistent TEER values around 400 $\Omega \cdot cm^2$, reflecting the optimal cell barriers for the transcellular transport studies of drug molecules (Stewart et al. 2012) (Fig. 1A left). The TEER values of the differentiated NHBE cells in the ALI condition were considerably higher than the Calu-3 cells with about 693 $\pm$ 46.6 $\Omega \cdot cm^2$ on day 6, reaching 967 $\pm$ 51.8 $\Omega \cdot cm^2$ on day 10 (Fig. 1A middle). Meanwhile, we tried the ALI cultures of the transformed cells, NL-20 in the inserts, and examined intactness of the NL-20 cell layers with the TEER measurements. In the NL-20 cells (Fig. 1A right), even with continuous cultures, the TEER values were maintained in a low level (~70 $\Omega \cdot cm^2$), not increasing to the level of 100 $\Omega \cdot cm^2$, i.e. typical TEER values in confluent MDCK (Madin Darby Canine Kidney) cell monolayers that have been widely used in drug transport studies (Taub et al. 2002).

Evaluation of cell layers as functional barriers for drug transport—As another way to confirm the cell intactness besides TEER measurements, the permeability of LY as a paracellular transport marker (Tsukazaki et al. 2004; Suresh et al. 2012) was used to evaluate the air-liquid interfaced cultures of the Calu-3, NHBE, or NL-20 cells as for the functional cell barriers suitable to drug permeability measurements for lung delivery. The LY permeability values (P_{eff}) for both directional transports (apical-to-basolateral (AP→BL); basolateral-to-apical (BL→AP)) in the Calu-3, NL-20 or NHBE cells are shown in Fig. 1B. No statistically significant difference was observed among the P_{eff} values of LY in the Calu-3 and NHBE cells for each directional transport (ANOVA with Tukey's multiple

comparison test, $p<0.05$). From these data, we found that the ALI cultures of the Calu-3 or NHBE cells formed intact cell barriers to ensure the usefulness for the transcellular drug transport studies. Unlike the Calu-3 and NHBE cells, NL-20 showed a high paracellular transport level in both directions (Fig. 1B).

Cytometric analysis

Variances in cell architectures on inserts—The TEER measurements and LY permeability values (Fig. 1) proved that tight junctions of NL-20 might not be fully developed on the porous support. Furthermore, we found that the differentiated NHBE cells and the Calu-3 cells had much higher TEER values than the NL-20 cells, suggesting intact cell layer formations. The TEER values in the NHBE cells were much higher than those in the Calu-3 cell cultures. In order to address the issues of different cell layer formation on porous supports, we examined these bronchial cells in the Transwell™ inserts by confocal fluorescent 3D imaging throughout the days of the ALI cultures. Suborganelles, such as cell nuclei, lysosomes or mitochondria, were visualized after the cells in the Transwell™ inserts were incubated with the dye mixtures containing HOE (blue) staining cell nuclei, LTG (green) for lysosomes, and MTR (red) for mitochondria (Fig. 2). Then, those images were analyzed by MetaMorph software to obtain morphometric parameters (cell area, height, and cell volume) (Fig. 3). Comparison of the stained patterns (Fig. 2) suggests that these cells showed a different intracellular accumulation or distribution of dye molecules. LTG accumulation in the Calu-3 and NL-20 cells was patchy and heterogeneous, while top cell layers of NHBE showed punctate and dispersed LTG-associated vesicles. When cell layer thicknesses seen in the xz plane images in Fig. 2 were compared with the cell height measurements in Fig. 3, cell layer thickness of Calu-3 was similar to the cell height, reflecting a consistent formation of cell monolayers during the cultures under the ALI conditions. On the other hand, NL-20 showed a 2- to 3-fold larger cell layer thickness developed from day 6 until day 10 than that on day 3. NHBE showed an about 2-fold larger cell layer thicknesses from day 6 until day 10, as compared to the layer thickness on day 3.

In the case of the NHBE cells, cell morphologies were different in the top and bottom cell layers (Fig. 3A). Cell heights in the NHBE bottom layers reflect mixed cell shapes of cuboidal and columnar cells, ranging from 6 to 13 μm. Top layers had smaller cell heights with the average of 7.63 μm ($\pm$ 0.68), 6.79 μm ($\pm$ 1.32), and 6.84 μm ($\pm$ 1.50) on days 6, 8, and 10, respectively. Bottom cells in NHBE on day 3 had a smaller cell volume than those on different days ($p<0.01$), reflecting that NHBE on day 3 might not be fully differentiated yet. Cell volume of the bottom cells on days 6, 8, and 10 were 5531 μm^3 ($\pm$ 865), 5311 μm^3 ($\pm$ 1164), and 5138 μm^3 ($\pm$ 853), respectively, but those of top cells were larger: 8557 μm^3 ($\pm$ 1108), 9327 μm^3 ($\pm$ 485) and 9312 μm^3 ($\pm$ 732) on average, respectively. The morphological parameters were consistent with the cell morphologies in the confocal images (Fig. 2A and 3A), showing that the NHBE bottom cells are more cuboidal and columnar, while top cells are more squamous.

On day 3, NL-20 showed a sparse distribution of cells in the cell layers. After day 4, the NL-20 cells started to form cell multilayers, but showed consistent cell morphologies of cuboidal shapes in top and bottom cell layers throughout the days of cultures (Fig. 2B).

Comparison of the top or bottom cell layers suggests that the NL-20 cells appeared to be cuboidal-shaped cells consistently through the cell layers with much smaller (ca. 4.6-fold difference) volume to the NHBE, and a relatively smaller volume (1.6-fold difference on average) to the Calu-3 (Fig. 3A, B, and C). Relatively, the NHBE on top or bottom layers and the Calu-3 monolayers showed larger variances in cell morphologies than the NL-20 cell layers, which suggests that the NHBE and Calu-3 cells would be well-differentiated bronchial cell types including heterogeneous cell phenotypes, such as ciliated, goblet, and/or basal cells, as shown in cell distributions of the airways *in vivo* (Gruenert et al. 1995; Ehrhardt et al. 2008). Previous studies have reported that respiratory epithelial cell types become composed of varied cell populations, as they undergo cell differentiation in a culture system (Berube et al. 2010). On day 3, the Calu-3 cells had imperfect cell intactness with sparse cuboidal-shaped cells on the membrane (see xz planes in Fig. 2C). After day 6, columnar cells of Calu-3 became compact with the neighboring cells. After day 3, the Calu-3 cells developed intact cell monolayers with cuboidal and columnar cell types and maintained cell monolayers throughout the cultures (Fig. 3C).

Therefore, differentiated NHBE cells formed cell multilayers with high intactness, while the transformed NL-20 cells developed cell multilayers with low intactness with disordered cell aggregations with dying off after day 30. Overall, the ALI cultures of the Calu-3 cells formed intact cell monolayers without disordered architectures, displaying consistent morphologies to become an appropriate cell model for drug transport studies.

Intracellular accumulation measurements of fluorescent probes—In the next step, fluorescent probes such as LTG or MTR have been used as model compounds to investigate intracellular retention across the cell layers in different human bronchial cell types. In the NHBE multilayers, throughout the ALI cultures, both dye molecules (MTR and LTG) showed a higher retention in the top cells than in the bottom cells, with decreased transport rates of those molecules across the intact cell layers (Fig. 4A). In terms of the degrees of transport across the NHBE cell multilayers, LTG appeared to be easily transported across the bottom cell layers relative to MTR. In the case of the NL20 multilayers between days 6 and 8, over 90 % of MTR retained in the top cell layers while LTG was easily penetrated through the bottom cell layers (Fig. 4B). In the Calu-3 cell monolayers, MTR showed a higher cell-associated accumulation than LTG, suggesting a higher LTG transport across monolayer and porous membrane in the insert (Fig. 4C).

The difference examined from microscopic transport experiments with the probes may be related with the different physicochemical properties of MTR and LTG. The molecular weight of MTR is larger than that of LTG, whereas the lipophilicity of MTR is lower than that of LTG. In the physiological pH environment of medium, MTR with a lower pKa can be confined to the intracellular compartment of the top cell layer due to the existence of more ionized MTR molecules. Therefore, under this pH condition, LTG molecules with a higher lipophilicity than that of MTR could be easily transported across cell layers and membrane pores. In addition, when the NHBE and NL-20 multilayers were compared throughout days of cultures, NHBE multilayers consistently showed a high intactness with a low MTR and LTG transport across the bottom cell layers. Meanwhile, the NL-20 multilayers after day 10 under the ALI conditions showed more MTR transport across cell

layers with a lower MTR accumulation in the top and bottom cells than the NL-20 cells in earlier days of cultures, providing further evidence on that the NL-20 cells became disorganized with loose intactness across cell layers after day 10.

Discussion

Cell model establishment can provide a simple and cheap experimental system for drug transport and metabolism studies. Furthermore, it can also facilitate mechanistic studies about ADMETox (absorption, distribution, metabolism (transporters or enzymes), elimination, and toxicity) profiles of drug molecules (Li 2001; Szakacs et al. 2008). Therefore, an investigation of biophysical properties of airway epithelial cell candidates is meaningful in terms of establishing appropriate cell models for studying pharmacokinetic profiles of inhaled drug molecules. Our results suggest that three human lung epithelial cell types, NHBE, NL-20, and Calu-3, have different cell morphologies and architectures on porous polyester membranes, developing different cell intactness (tight junctions) during the ALI condition culture. Moreover, when comparing the stained patterns with dye molecules, these cells demonstrated a different intracellular accumulation or distribution of small molecules. Overall, our functional data (TEER values and LY permeability) and the imaging analysis results confirm that the Calu-3 cells developed intact cell monolayers with columnar cell types after day 6 and maintained confluent cell barriers on porous membranes throughout the culture period.

When cultured in the ALI conditions on the porous polyester membrane, the Calu-3 cells showed well-developed tight junctions with cell monolayers and consistent behaviors in transport/retention of dye small molecules during cultures, suggesting that the Calu-3 cells have desirable properties as cell model for drug transport studies. Meanwhile, the differentiated NHBE cells developed tight junctions with the highest TEER values, but formed cell multilayers, which is different from the *in vivo* lung with bronchial cell monolayers. Finally, NL-20 did not show intactness in cell layers throughout the culture period, suggesting that NL-20 might not be a suitable cell model for drug transport studies. Even though the NL-20 cells were originally transformed from normal human lung cells, they showed quite different behaviors (i.e., growing patterns on the membranes) or morphologies having cell sizes or volumes different from those of the NHBE cells. Initially, as a new strain established by transfecting normal human bronchial epithelial cells with SV40 virus, NL-20 has been reported to be non-tumorigenic with no mutations in K-ras codons and no DNA amplification for c-myc (Schiller et al. 1994). Also, these cell types were reported not to have activation of dominant oncogenes or inactivation of tumor suppressor genes widely found in human lung cancers (Schiller et al. 1994). Even though NL-20 has been recognized as a useful non-tumorigenic, normal cell model for studying carcinogenesis of lung cancers (Yang et al. 2012), the results of the present study suggest that NL-20 does not have physical characteristics of a functional epithelial barrier which is a requirement for a cell model for drug transport studies.

Confocal microscope imaging enabled us to investigate cell-to-cell or cell-to-membrane interactions in the architectures of the cells grown on the nucleopore membrane in different growth conditions (i.e., different pore sizes of membranes (0.4 or 3 μm)) with 3D dimension

by Z-stacks. When the cells were grown on the membranes with 0.4 μm-sized pores under the ALI conditions as described above, the Calu-3 cells formed tight, packed monolayers of cuboidal or columnar architecture as monolayers. In contrast to Calu-3 showing monolayers, NHBE in differentiation medium formed tight multilayered structures and NL-20 cells were unstable, forming stacked, multilayered structures starting on day 4 after seeding. Compared to our results on the membranes with 0.4 μm-sized pores, when the cells were cultured on membranes with the larger pore size (3 μm), NHBE cells were dying off after day 6 and NL-20 did not form multilayers (see Fig. S1 in the online supplementary data). Only the Calu-3 cells could form intact cell monolayers on these membranes with larger pores. This difference might result from different protein expressions on basolateral membrane, which could influence cellular interaction with the extracellular matrix (Louvard et al. 1992; O'Brien et al. 2002).

In terms of cell-to-cell interactions under growing conditions in the inserts, the scatter plots in Fig. S2 and S3 (see the online supplementary data) show the coupled relationships among the cytometric parameters. Throughout the days of the cultures under the ALI conditions, NHBE in the top layers showed increasing patterns of cell areas and volumes with shorter cell heights, whereas NHBE in the bottom layers showed rather consistency in cell areas, heights, and volumes. The NHBE cell volume was proportionally coupled with the cell area (Fig. S2). Meanwhile, there was apparently an inverse relationship between the cell area and cell height in the case of the Calu-3 and NL-20 cells through the days of culture (days 3, 6, 8, and 10) (Fig. S3). This relationship suggests that cell morphologies might be affected by increasing neighboring cells in the physically defined space during the culture (Vunjak-Novakovic and Freed 1998). On day 3, the NL20 cells were not compact with neighboring cells, resulting in a larger cell area with a shorter cell height. Throughout the days of the ALI cultures, the NL-20 top and bottom layers became composed of homogeneous cuboidal-shaped cells with little variance in cell volumes, with smaller cell areas, and larger cell heights than those of the cells on day 3 (Fig. S3A and S3B).

After 30-min transport of dye molecules, integrated intensity of MTR showed clear differences in the extent of bioaccumulation amongst the cell layers of different cell types after day 6 of the ALI cultures (level: NL-20 top cells < Calu-3 < NHBE top cells) (Fig. 4). For the integrated intensity of MTR, the NHBE top cells showed a 3.1-fold larger intensity than the Calu-3 throughout the cultures. For the integrated intensity of LTG, the NHBE cells in the top cell layers showed a 2.0-fold larger intensity than Calu-3. This could suggest more accumulations of small molecules in the NHBE cells than in the Calu-3 cells. This finding on the differences in transport/retention of fluorescent molecules in airway cell types might be related to different expression levels of cellular components involved in drug accumulation or uptake mechanism (Casartelli et al. 2003; Dobson and Kell 2008). Other reports have shown that NHBE and Calu-3 have different ion regulatory mechanisms (i.e., Cl^- channel) in the plasma membranes (Shen et al. 1994; Szkotak et al. 2003), as well as different expression levels of proteins (i.e., tubulins or mucins) on cell surfaces (Guzman et al. 1996; Huang et al. 2010; Stewart et al. 2012). Differences in expression levels or types of cellular factors could induce variations in local microenvironment on cell surface, finally resulting in different bioaccumulation or transport of drug molecules across these different cell types.

In conclusion, our results demonstrate that a new strategy of combination with chemical transport assays and quantitative microscopic investigations could be used to provide meaningful information about appropriate cell types or days of cell cultures on the porous supports, the specialized experimental setting for drug transport studies. Even though the NL-20 cells were originally transformed from normal human lung cells, they showed quite different behaviors (i.e., growing patterns on the membranes) or morphologies having cell sizes or volumes different from those of the NHBE cells. Among the three studied types of bronchial cells, the Calu-3 cells showed optimal cytometric properties as functional cell barriers for the lung-targeted drug transport studies. Ultimately, our experimental design could be used to screen various cell lines or primary cells obtained from different locations of the respiratory system to select appropriate *in vitro* cell models for the pharmacokinetic studies with the inhaled drug molecules.

Supplementary Material

Refer to Web version on PubMed Central for supplementary material.

Acknowledgments

References

Agu RU, Ugwoke MI, Armand M, Kinget R, Verbeke N. The lung as a route for systemic delivery of therapeutic proteins and peptides. Respir Res. 2001; 2:198–209. [PubMed: 11686885]

Astashkina A, Mann B, Grainger DW. A critical evaluation of in vitro cell culture models for high-throughput drug screening and toxicity. Pharmacol Ther. 2012; 134:82–106. [PubMed: 22252140]

Berube K, Prytherch Z, Job C, Hughes T. Human primary bronchial lung cell constructs: the new respiratory models. Toxicology. 2010; 278:311–318. [PubMed: 20403407]

Bhadriraju K, Chen CS. Engineering cellular microenvironments to improve cell-based drug testing. Drug Discov Today. 2002; 7:612–620. [PubMed: 12047872]

Borchard G, Cassara ML, Roemele PE, Florea BI, Junginger HE. Transport and local metabolism of budesonide and fluticasone propionate in a human bronchial epithelial cell line (Calu-3). J Pharm Sci. 2002; 91:1561–1567. [PubMed: 12115854]

Casartelli A, Bonato M, Cristofori P, Crivellente F, Dal Negro G, Masotto I, Mutinelli C, Valko K, Bonfante V. A cell-based approach for the early assessment of the phospholipidogenic potential in pharmaceutical research and drug development. Cell Biol Toxicol. 2003; 19:161–176. [PubMed: 12945744]

Cozens AL, Yezzi MJ, Yamaya M, Steiger D, Wagner JA, Garber SS, Chin L, Simon EM, Cutting GR, Gardner P, Friend DS, Basbaum CB, Gruenert DC. A transformed human epithelial cell line that retains tight junctions post crisis. In Vitro Cell Dev Biol. 1992; 28A:735–744. [PubMed: 1282914]

Dobson PD, Kell DB. Carrier-mediated cellular uptake of pharmaceutical drugs: an exception or the rule? Nat Rev Drug Discov. 2008; 7:205–220. [PubMed: 18309312]

Ehrhardt, C.; Forbes, B.; Kim, K-J. In vitro models of the tracheo-bronchial epithelium. In: Ehrhardt, C.; Kim, K-J., editors. Drug absorption studies. Springer; New York: 2008. p. 235-257.

Florea BI, Cassara ML, Junginger HE, Borchard G. Drug transport and metabolism characteristics of the human airway epithelial cell line Calu-3. J Control Release. 2003; 87:131–138. [PubMed: 12618029]

Forbes B, Ehrhardt C. Human respiratory epithelial cell culture for drug delivery applications. Eur J Pharm Biopharm. 2005; 60:193–205. [PubMed: 15939233]

Frixione E, Lagunes R, Ruiz L, Urban M, Porter RM. Actin cytoskeleton role in the structural response of epithelial (MDCK) cells to low extracellular Ca^{2+} J Muscle Res Cell Motil. 2001; 22:229–242. [PubMed: 11763195]

Gonda I. Systemic delivery of drugs to humans via inhalation. J Aerosol Med. 2006; 19:47–53. [PubMed: 16551214]

Grainger CI, Greenwell LL, Lockley DJ, Martin GP, Forbes B. Culture of Calu-3 cells at the air interface provides a representative model of the airway epithelial barrier. Pharm Res. 2006; 23:1482–1490. [PubMed: 16779708]

Gray TE, Guzman K, Davis CW, Abdullah LH, Nettesheim P. Mucociliary differentiation of serially passaged normal human tracheobronchial epithelial cells. Am J Respir Cell Mol Biol. 1996; 14:104–112. [PubMed: 8534481]

Gruenert DC, Finkbeiner WE, Widdicombe JH. Culture and transformation of human airway epithelial cells. Am J Physiol. 1995; 268:L347–360. [PubMed: 7900815]

Guzman K, Gray TE, Yoon JH, Nettesheim P. Quantitation of mucin RNA by PCR reveals induction of both MUC2 and MUC5AC mRNA levels by retinoids. Am J Physiol. 1996; 271:L1023–1028. [PubMed: 8997274]

Huang TW, Chan YH, Cheng PW, Young YH, Lou PJ, Young TH. Increased mucociliary differentiation of human respiratory epithelial cells on hyaluronan-derivative membranes. Acta Biomater. 2010; 6:1191–1199. [PubMed: 19716445]

Irvine JD, Takahashi L, Lockhart K, Cheong J, Tolan JW, Selick HE, Grove JR. MDCK (Madin-Darby canine kidney) cells: A tool for membrane permeability screening. J Pharm Sci. 1999; 88:28–33. [PubMed: 9874698]

Li AP. Screening for human ADME/Tox drug properties in drug discovery. Drug Discov Today. 2001; 6:357–366. [PubMed: 11267922]

Lin H, Li H, Cho HJ, Bian S, Roh HJ, Lee MK, Kim JS, Chung SJ, Shim CK, Kim DD. Air-liquid interface (ALI) culture of human bronchial epithelial cell monolayers as an in vitro model for airway drug transport studies. J Pharm Sci. 2007; 96:341–350. [PubMed: 17080426]

Louvard D, Kedinger M, Hauri HP. The differentiating intestinal epithelial cell: establishment and maintenance of functions through interactions between cellular structures. Annu Rev Cell Biol. 1992; 8:157–195. [PubMed: 1476799]

O'Brien LE, Zegers MM, Mostov KE. Opinion: Building epithelial architecture: insights from three-dimensional culture models. Nat Rev Mol Cell Biol. 2002; 3:531–537. [PubMed: 12094219]

Patton JS, Byron PR. Inhaling medicines: delivering drugs to the body through the lungs. Nat Rev Drug Discov. 2007; 6:67–74. [PubMed: 17195033]

Sachs LA, Finkbeiner WE, Widdicombe JH. Effects of media on differentiation of cultured human tracheal epithelium. In Vitro Cell Dev Biol Anim. 2003; 39:56–62. [PubMed: 12892528]

Schiller J, Sabatini L, Bittner G, Pinkerman C, Mayotte J, Levitt M, Meisner L. Phenotypic, molecular and genetic-characterization of transformed human bronchial epithelial-cell strains. Int J Oncol. 1994; 4:461–470. [PubMed: 21566947]

Schiller JH, Bittner G, Oberley TD, Kao C, Harris C, Meisner LF. Establishment and characterization of a SV40 T-antigen immortalized human bronchial epithelial cell line. In Vitro Cell Dev Biol. 1992; 28A:461–464. [PubMed: 1522038]

Shah P, Jogani V, Bagchi T, Misra A. Role of Caco-2 cell monolayers in prediction of intestinal drug absorption. Biotechnol Prog. 2006; 22:186–198. [PubMed: 16454510]

Shen BQ, Finkbeiner WE, Wine JJ, Mrsny RJ, Widdicombe JH. Calu-3: a human airway epithelial cell line that shows cAMP-dependent Cl^- secretion. Am J Physiol. 1994; 266:L493–501. [PubMed: 7515578]

Stewart CE, Torr EE, Mohd Jamili NH, Bosquillon C, Sayers I. Evaluation of differentiated human bronchial epithelial cell culture systems for asthma research. J Allergy. 2012; 2012:943982.

Suresh MV, Wagner MC, Rosania GR, Stringer KA, Min KA, Risler L, Shen DD, Georges GE, Reddy AT, Parkkinen J, Reddy RC. Pulmonary administration of a water-soluble curcumin complex

reduces severity of acute lung injury. Am J Respir Cell Mol Biol. 2012; 47:280–287. [PubMed: 22312018]

Szakacs G, Varadi A, Ozvegy-Laczka C, Sarkadi B. The role of ABC transporters in drug absorption, distribution, metabolism, excretion and toxicity (ADME-Tox). Drug Discov Today. 2008; 13:379–393. [PubMed: 18468555]

Szkotak AJ, Man SF, Duszyk M. The role of the basolateral outwardly rectifying chloride channel in human airway epithelial anion secretion. Am J Respir Cell Mol Biol. 2003; 29:710–720. [PubMed: 12777250]

Taub ME, Kristensen L, Frokjaer S. Optimized conditions for MDCK permeability and turbidimetric solubility studies using compounds representative of BCS classes I–IV. Eur J Pharm Sci. 2002; 15:331–340. [PubMed: 11988394]

Tsukazaki M, Satsu H, Mori A, Sugita-Konishi Y, Shimizu M. Effects of tributyltin on barrier functions in human intestinal Caco-2 cells. Biochem Biophys Res Commun. 2004; 315:991–997. [PubMed: 14985110]

Volpe DA. Variability in Caco-2 and MDCK cell-based intestinal permeability assays. J Pharm Sci. 2008; 97:712–725. [PubMed: 17542022]

Vunjak-Novakovic G, Freed LE. Culture of organized cell communities. Adv Drug Deliv Rev. 1998; 33:15–30. [PubMed: 10837650]

Wu R, Zhao YH, Chang MM. Growth and differentiation of conducting airway epithelial cells in culture. Eur Respir J. 1997; 10:2398–2403. [PubMed: 9387971]

Yang J, Lan H, Huang X, Liu B, Tong Y. MicroRNA-126 inhibits tumor cell growth and its expression level correlates with poor survival in non-small cell lung cancer patients. PLoS One. 2012; 7:e42978. [PubMed: 22900072]

Yu JY, Zheng N, Mane G, Min KA, Hinestroza JP, Zhu H, Stringer KA, Rosania GR. A cell-based computational modeling approach for developing site-directed molecular probes. PLoS Comput Biol. 2012; 8:e1002378. [PubMed: 22383866]
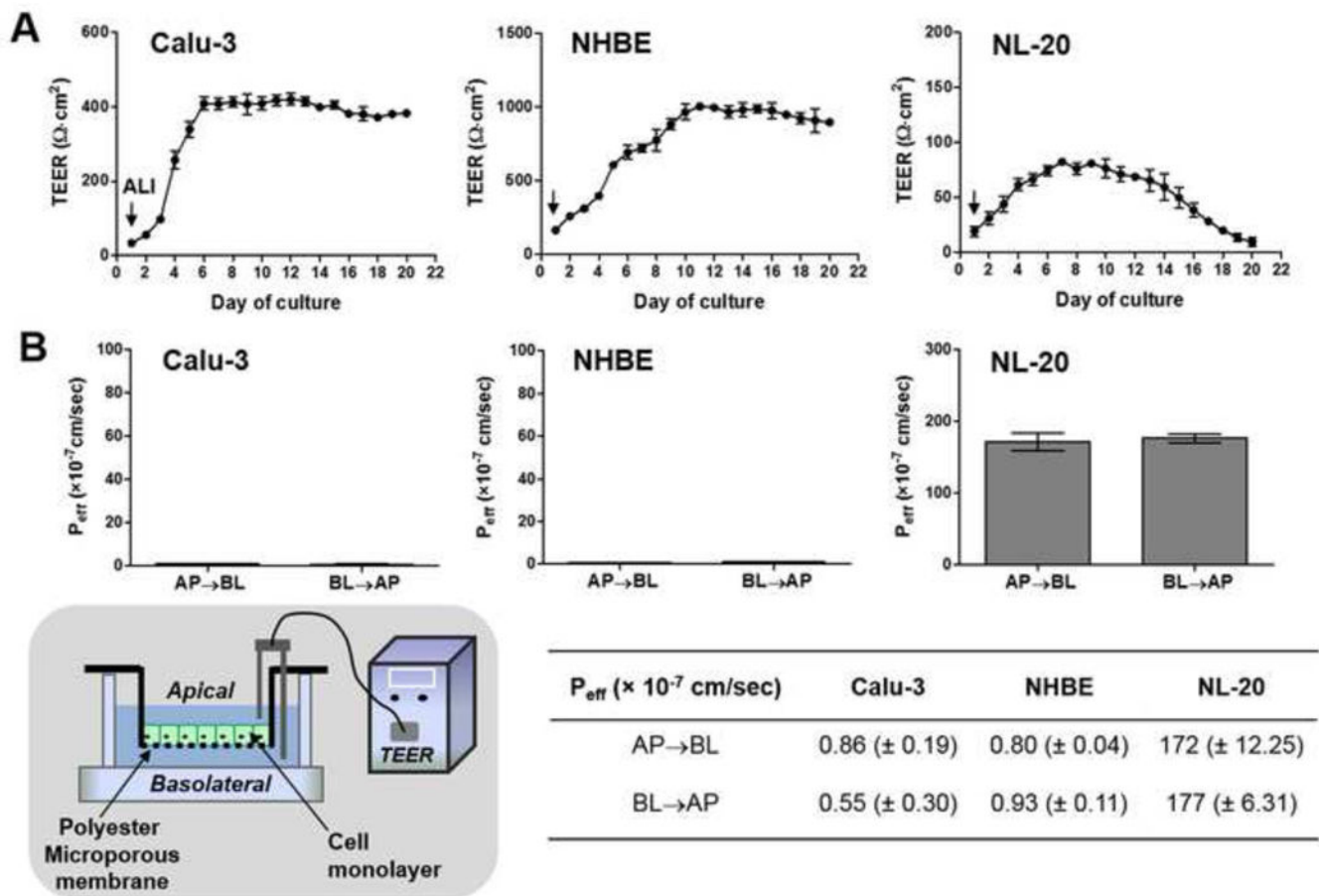
Fig. 1.
Integrity test of cell layers grown on the porous supports. (A) The TEER measurements of different lung epithelial cells (Calu-3, NHBE, NL-20 cells) throughout the air-liquid interface (ALI) cultures (until day 20). (B) LY (Lucifer yellow) permeability values (P_{eff} ($\times$ 10^{-7} cm/sec)) for AP→BL (apical-to-basolateral) or BL→AP (basolateral-to-apical) transport of each lung epithelial cell type in Transwell™ cultures on day 8 under the ALI conditions. Mean values with standard deviation (mean ± S.D., n=3) of permeability coefficients are displayed in the incorporated table, corresponding to the bar graphs in (B). The schematic diagram shows measuring TEER in the experimental settings with the inserts.
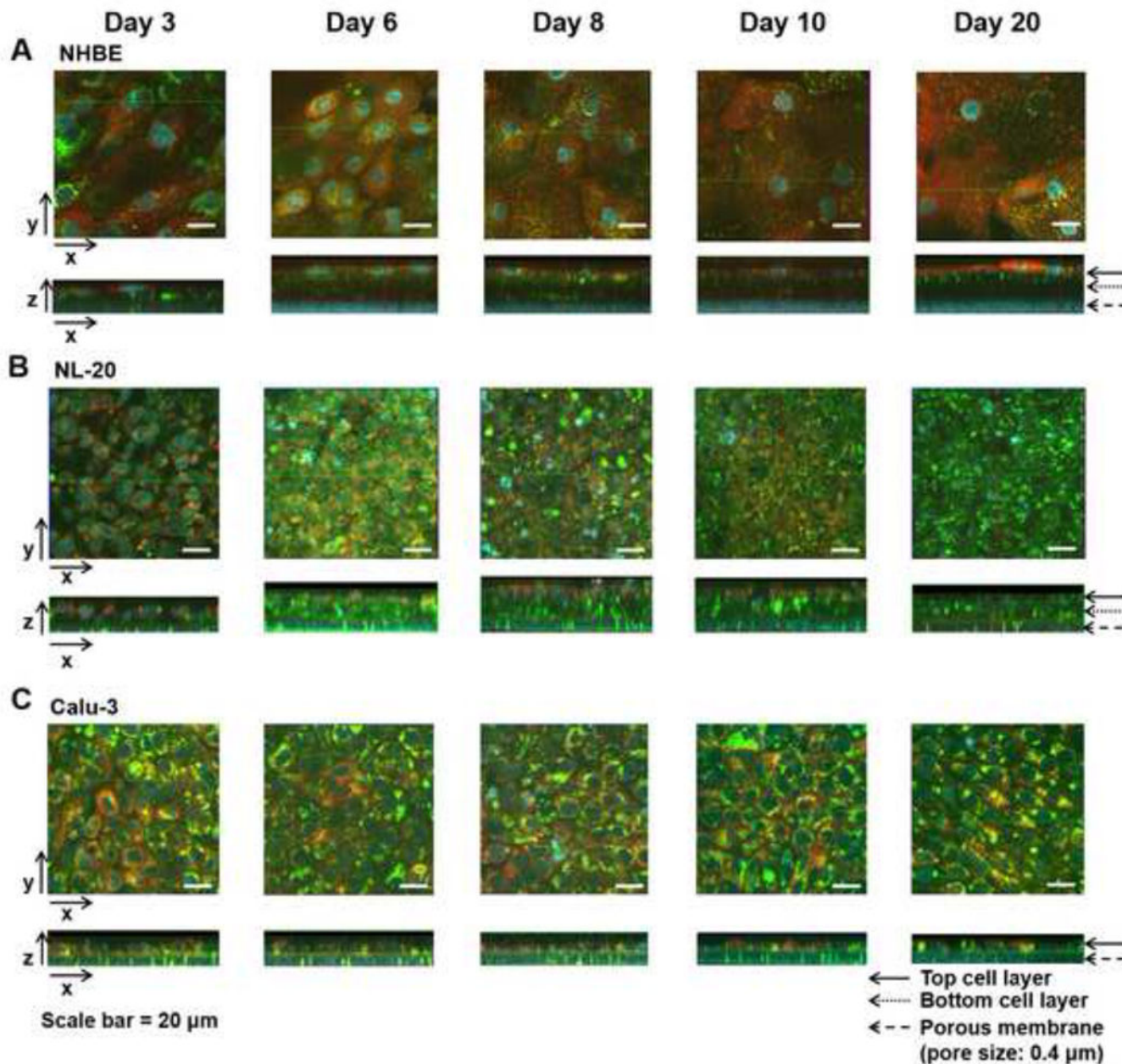
Fig. 2.
Confocal fluorescence microscopic images of three different human lung epithelial cells ((A) NHBE, (B) NL-20, (C) Calu-3) after dye transport on different days of cultures (days 3, 6, 8, 10, and 20) under the ALI conditions. The cell layers in the inserts were incubated with the mixture of cell-permeant probes (MTR, Hoe, and LTG) on the apical side and then underwent confocal analyses with Zeiss LSM 510 confocal microscopy. Hoechst 33342 (Hoe) was used for staining cell nuclei (blue); LysoTracker® Green DND-26 (LTG) for lysosomes (green), MitoTracker® Red (MTR) for mitochondria (red). Three axes (x, y, and z) are depicted with the arrows in the images processed by Zeiss LSM browser. Cell architectures in the inserts are apparently shown in xz planes with the indications of the

arrows for the top, bottom cell layer, and the porous membrane (pore size: 0.4 μm). Scale bar = 20 μm.
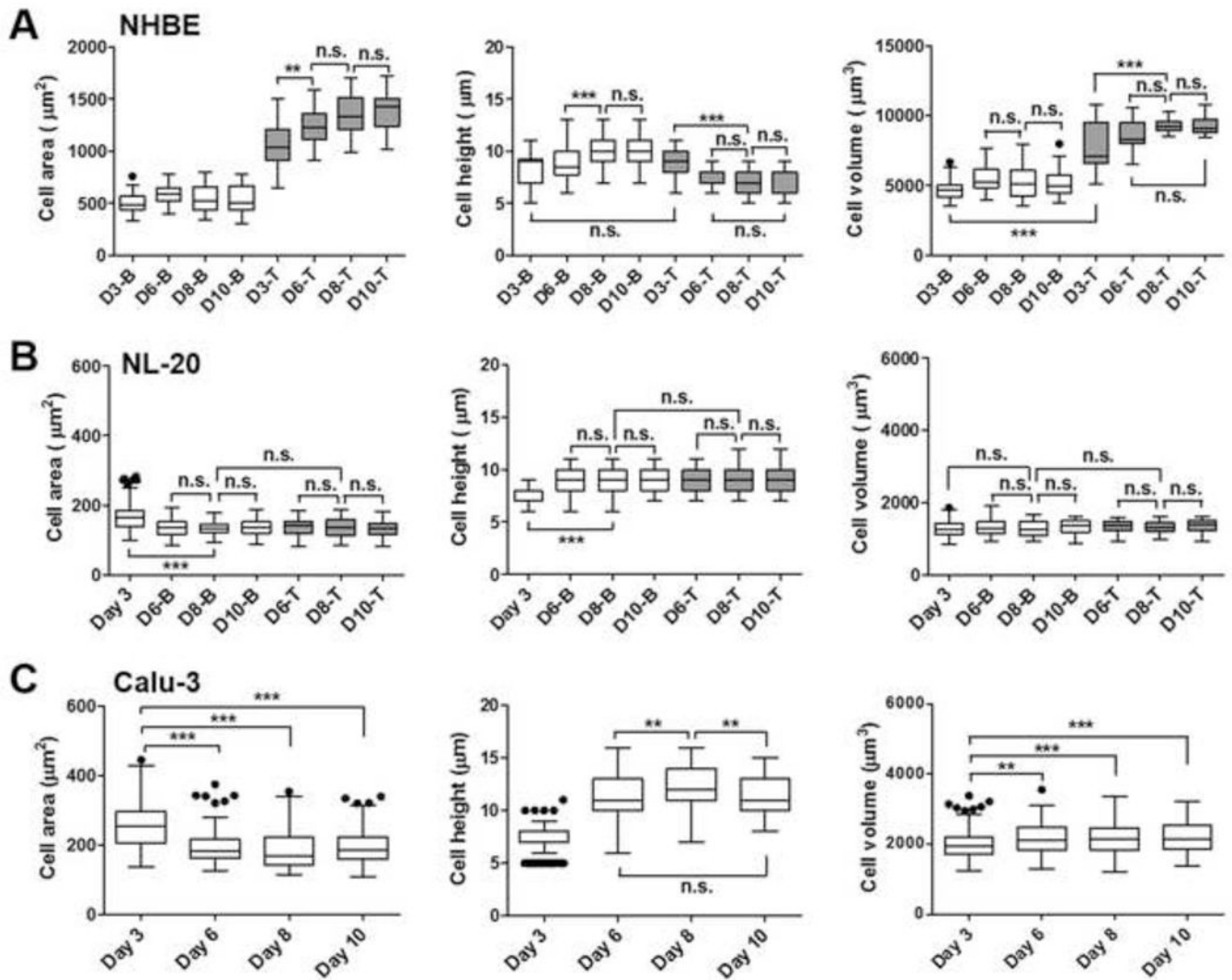
Fig. 3.
Variations in the morphological parameters of three different human lung epithelial cells
((A) NHBE, (B) NL-20, (C) Calu-3) in different days of cultures under the ALI conditions.
Cell area (μm^2), height (μm), and volume (μm^3) on days 3, 6, 8, and 10 (D3, D6, D8, D10)
are displayed for top (T) or bottom (B) cell layers in NHBE or NL-20 and the Calu-3 cell
monolayer after image analyses by Metamorph software. Box-whisker plots showing
median and interquartile range with whisker ends are depicted after the post-hoc multiple
mean comparison (Tukey's test, $p<0.05$). Statistical analyses were performed with Tukey's
multiple comparison tests with the 5% significance level. n.s.=not significant, *$p<0.05$,
**$p<0.001$, ***$p<0.0001$.
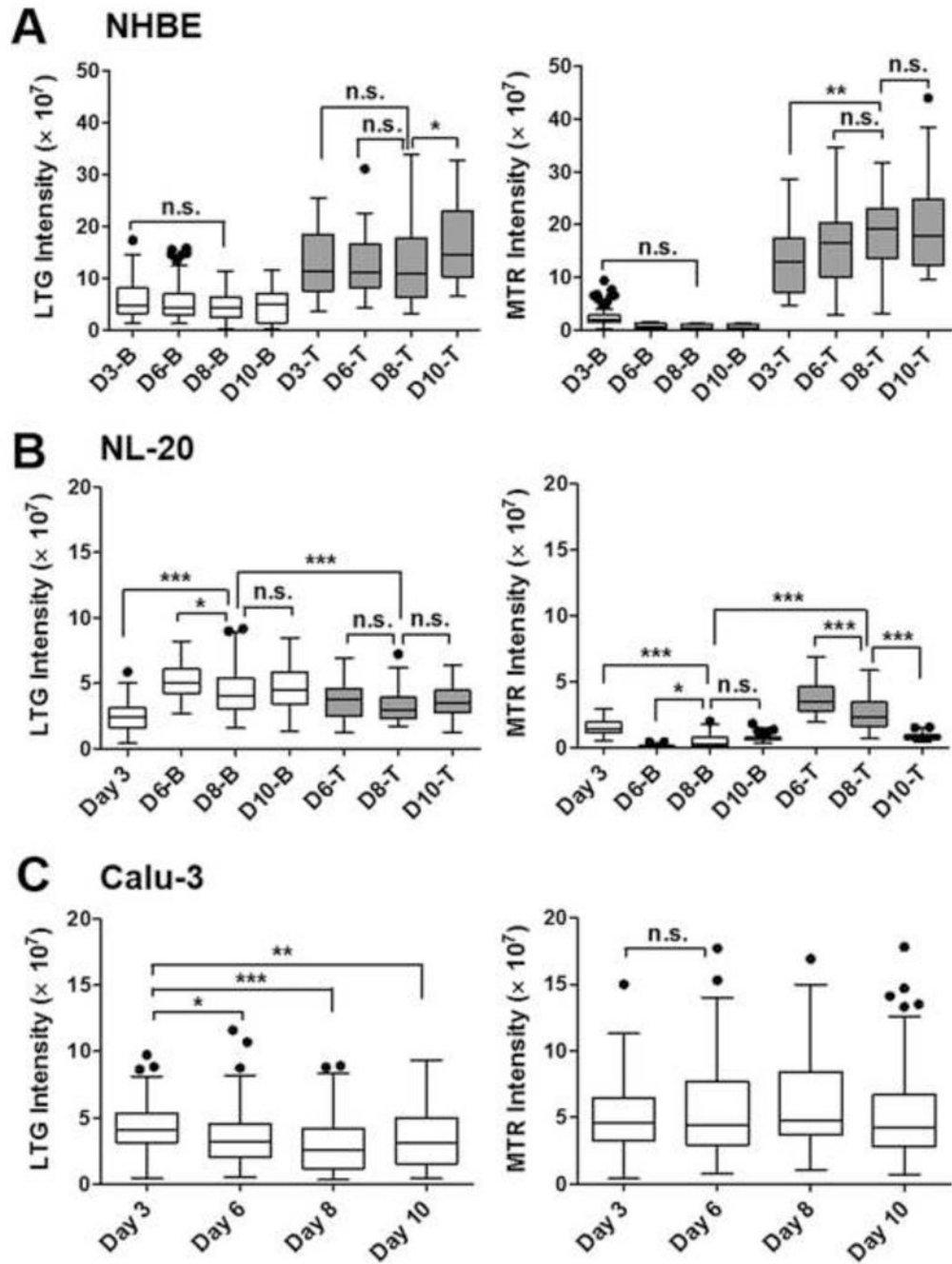
Fig. 4.
Fluorescence intensity measurements of probes staining suborganelles in three different human lung epithelial cell-types ((A) NHBE, (B) NL-20, (C) Calu-3) on different days of cultures under the ALI conditions. Integrated intensity values of LysoTracker® Green DND-26 (LTG) and MitoTracker® Red (MTR) were measured for top or bottom cell layers in NHBE or NL-20 and the Calu-3 cell monolayer on days 3, 6, 8, and 10 by the Metamorph. Box-whisker plots showing median and interquartile range with whisker ends are depicted after the post-hoc multiple mean comparison (Tukey's test, $p < 0.05$). Statistical

analyses were performed with Tukey's multiple comparison test with the 5% significance level. n.s.=not significant, $*p<0.05$, $**p<0.001$, $***p<0.0001$.